Improving Mechanical Properties of Nextel 610™-Reinforced Al-224 Alloy Through θ Phase Precipitation at the Fiber/Matrix Interface: Kinetics of the Precipitation Process

M.L. Seleznev, J.A. Cornie, and F.A. Armatis, Jr.

Earlier studies of Nextel 610 (seeded sol-gel-derived Al_2O_3 multifilament tow developed by 3M) reinforced Al-224.2 composite panels manufactured by pressure infiltration casting revealed interface delamination as a result of precipitation of the equilibrium θ precipitate and preferential growth at fiber/matrix interface sites. As a result, strengths as high as 91% of rule of mixtures (ROM) were observed. 75% ROM strengths were observed after extended heating at 350 °C and hence *in situ* coarsening of the interface θ precipitates. Transverse specimens displaying this still acceptable tensile strength exhibited values of 490 MPa (approaching that of wrought 2*xxx* alloys). This combination of high axial and transverse strengths from material in the same condition represents a significant improvement in this class of materials. This process is termed "discontinuously coated interfaces" (DCI™). In the present study, the kinetics of the coarsening process were measured at 350 and 400 °C using a new algorithm for the quantitative metallography determinations of the particle distribution at the interface. The interfacial θ coarsening kinetics follows a classical $t^{1/4}$ rate law. However, the particle size distribution is contrary to the theoretical predictions. Axial flexure tests on materials subjected to heat treatments at 350 and 400 °C producing close particle sizes result in similar flexure strengths. Thus, it has been demonstrated that the precipitate size and hence distribution at the interface is the most important factor controlling the mechanical properties of the composite.

Keywords
alumina fiber, interface, metal matrix composites, precipitation

1. Introduction

IT is widely recognized that the mechanical properties of composites are controlled by the structure and properties of the interfacial region between the fiber and matrix. Recent studies have demonstrated that interface delamination mechanisms can be used to decouple the reinforcing fibers from early damage due to stress concentrations near the interface such as adjacent broken fibers.[1] The delamination toughening mechanism is activated by decreasing the cohesive strength of the interface. Cohesive strength reductions generally are accomplished by CVD deposition of weak interface coatings onto the fiber surface prior to consolidation,[2] as effectively demonstrated for SCS-6 monofilament reinforcements for titanium alloys. In the authors' previous study,[3] an alternative approach to interface design based on *in situ* preferential coarsening of equilibrium precipitates at interfacial sites was demonstrated. The fiber/matrix interface was modified through an enhanced high-angle boundary precipitation mechanism in a Nextel 610 (seeded sol-gel-derived Al_2O_3 multifilament tow developed by 3M) reinforced classical Al-Cu (224.2) precipitation-hardening alloy. The present work focuses on kinetics of the precipitation reaction at 350 and 400 °C in the same composite material. The microstructural studies are correlated with mechanical properties of composite test coupons that have been given the same heat treatment.

M.L. Seleznev, J.A. Cornie, and **F.A. Armatis, Jr.,** Materials Processing Center, Massachusetts Institute of Technology, Cambridge, Massachusetts.

2. Experimental Design and Procedures

For the detailed description of Nextel 610 alumina fiber evaluation, matrix alloy, preform preparation, pressure infiltration casting, and scanning electron microscopy (SEM) techniques for interface microstructure evaluation, the reader is referred to Ref 3. The procedures and techniques not described there are as follows.

2.1 *Four-Point Bend Flexure Test*

The geometry of the test was designed according to ASTM Standard E-855-90. The span was 45 mm, and the distance between load application points was 30 mm. The cross section of the specimens was 6 by 1.35 mm.

2.2 *Microstructural Evaluation Procedures*

The microstructural features characterized in the present work were average precipitate size, area fraction, size distribution, and average nearest neighbor distance of $CuAl_2$ (θ) precipitates in the fiber/matrix interface region. All information was extracted from the SEM backscattered electron contrast

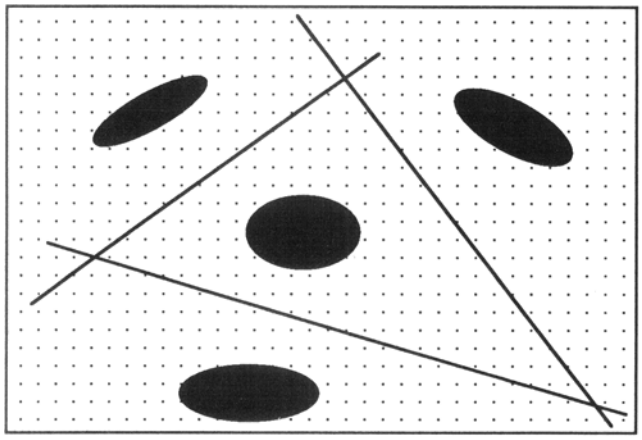

Fig. 1 Algorithm for the Dirichlet tessellation method of measuring interparticle distances.

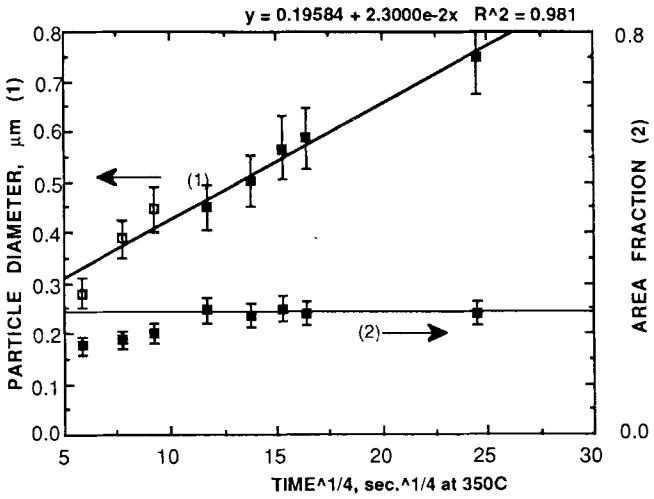

Fig. 2(a) Kinetics of interface precipitate growth in diameter (1) and area fraction of interface occupied by an Al_2Cu precipitate (2) at 350 °C.

images of a "diving fiber interface."[3] Nominally, eight photomicrographs at a magnification of 6000× were taken for each experimental point. The images were then digitized at 300 dots per inch, 256 gray level resolution, and subjected to computer image analysis.

Apart from standard image analysis routines, such as gray level discrimination and converting the image to binary form, it should be stressed that reproducible results are obtainable only if the proper techniques for treating SEM resolution uncertainties are applied. Because of SEM resolution limitations, the edges of particles, especially small particles, are not well defined. The image of a particle consists of the particle itself plus a vague boundary region. In this case, the gray level discrimination should be set in such a way as to define the particle including the entire boundary region. Then, a mathematical operation should be applied to exclude half of the vague boundary thickness.

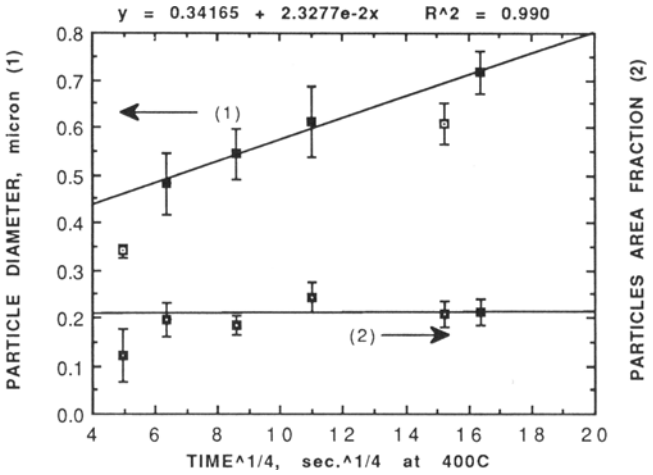

Fig. 2(b) Kinetics of interface precipitate growth in diameter (1) and area fraction of interface occupied by an Al_2Cu precipitate (2) at 400 °C.

The interface precipitates have a morphology that is not perfectly round. Nevertheless, to make the size distribution problem mathematically tractable, the size of the particle was presented as the diameter of the circle of the equal area.

The problem of defining the mean closest neighbor interparticle distance has been approached by several authors.[4,5] In Ref 4, the analytical approach to a monodispersed assembly of round particles of finite volume fraction was applied. In Ref 5, the computer analysis using Dirichlet tessellation of image area was used. However, unlike the case of round particles, analytical solutions of the problem cannot be applied readily to elliptical particles (which are not monodispersed). The computer analysis in Ref 5 does not provide the information needed in this study. It gives average center-to-center distance between neighboring particles rather than average free distance between particles. For that reason, the authors developed their own algorithm for computer analysis. The concept is presented in Fig. 1. The structure of an interface with precipitates is approximated by ellipses that correspond to the areas and orientations of the particles that they represent, as in Ref 5. Then, the network of points is overlaid onto the image. For each point, the shortest distance to neighboring ellipses is defined. As a result, the assemblies of the closest points is found for each ellipse. Averaging the distances between the ellipse and its closest points provides an estimate of half of the average distance between the particle border and the border of the Dirichlet region for this particle. Averaging this distance over all particles at the interface provides an estimate of the quarter of the mean interparticle free distance.

2.3 *Heat Treatment*

The interface precipitation reactions in this work were evaluated at 350 and 400 °C. Before heat treating samples at 350 and 400 °C, they were given a standard initial T7 heat treat condition consisting of an as-cast sample plus 4 h at 500 °C plus 25 h at 535 °C plus water quenching plus overaging 4 h at 200 °C.

3. Results and Discussion

3.1 *Kinetics of Coarsening of θ Precipitates at the Fiber/Matrix Interface*

The average particle size and area fraction at the interface as a function of time at 350 and 400 °C is presented in Fig. 2(a) and (b). The plot in Fig. 2(a) of area fraction of the fiber surface occupied by θ precipitates as a function of time at 350 °C shows a constant volume fraction after ~2 to 5 h. After that time, the solute no longer precipitates from the supersaturated solid solution, and the coarsening mechanisms predominate. Thus, the kinetics of the coarsening reaction should be related to times greater than 5 h at 350 °C. The plot of particle size versus time, $t^{1/4}$, is linear. This coincides with theoretical predictions for both precipitation and particle coarsening at grain boundaries or other high-angle boundaries.[6-8]

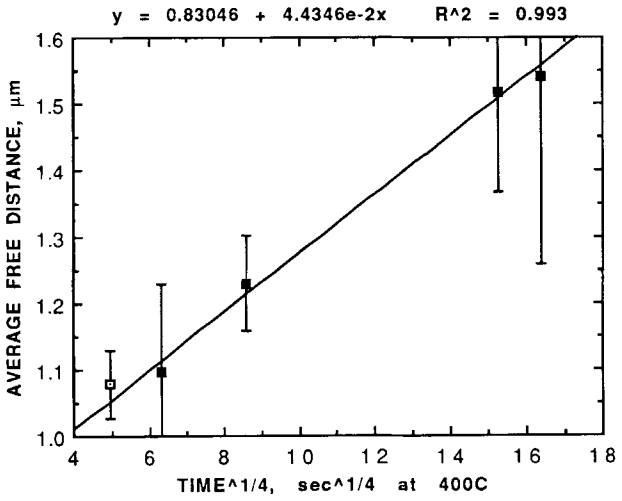

Fig. 3 Plot of the average distance between neighboring θ precipitates as a function of $t^{1/4}$ at 400 °C.

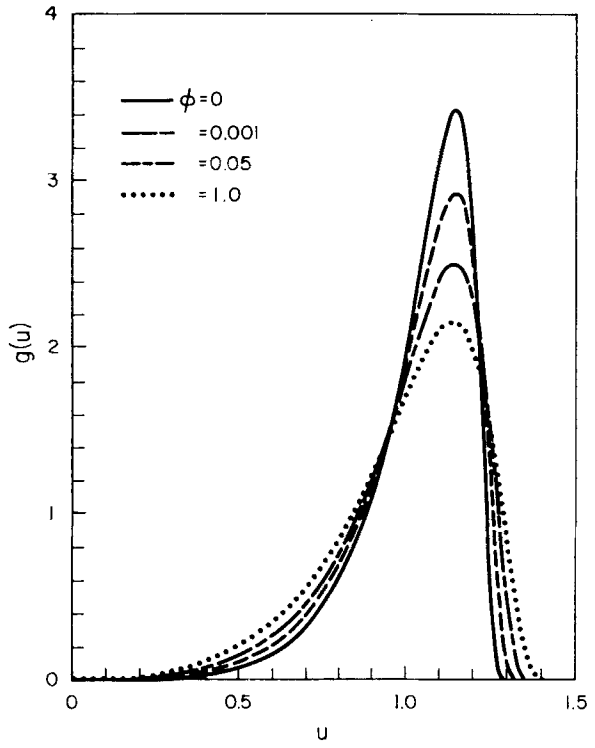

Fig. 4 Theoretical distribution function from Ardell[8] for different volume fractions of coarsening particles.

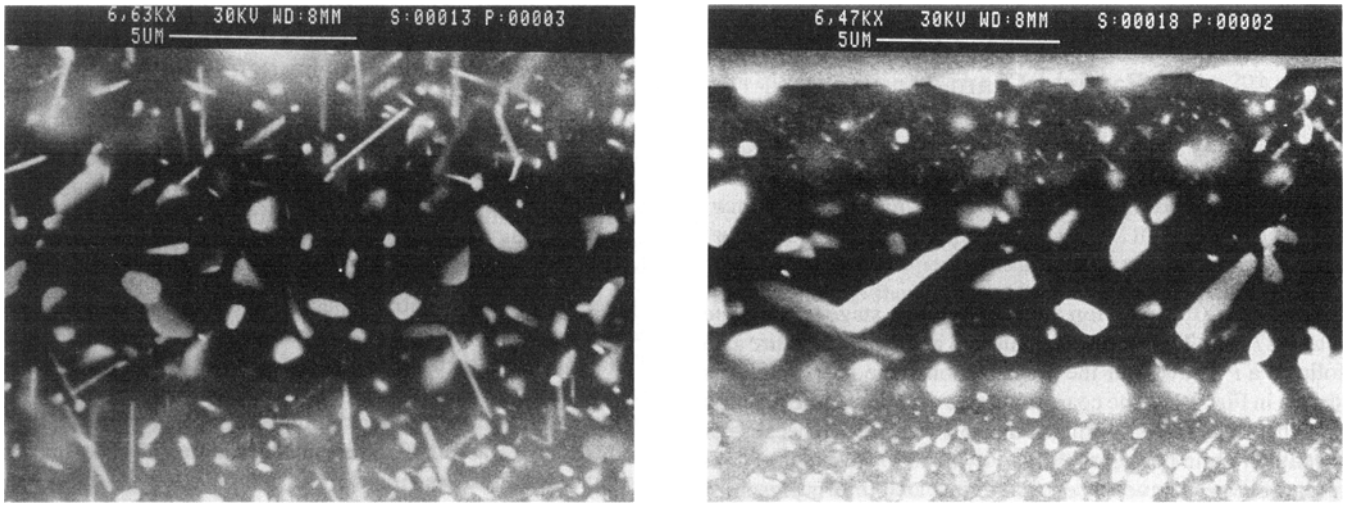

Fig. 5 Typical microstructures of interface region of Nextel-reinforced Al-224.2 after heat treating to T7 plus 27 min (a) and for 20 h (b) at 400 °C.

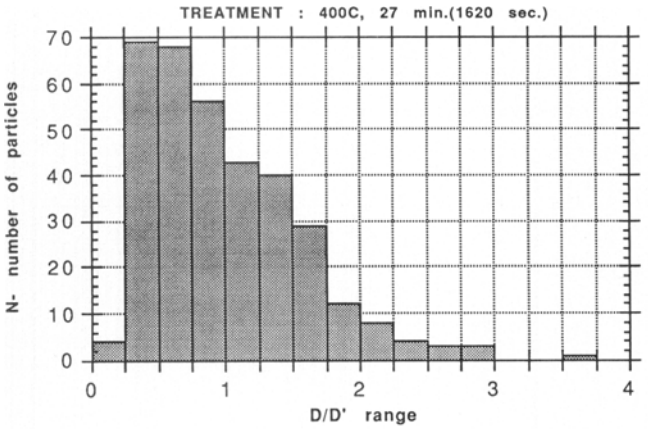

Fig. 6(a) Particle size distribution at alumina fiber interface region of Nextel 610-reinforced Al-224.2 alloy after heat treating to T7 plus 27 min at 400 °C.

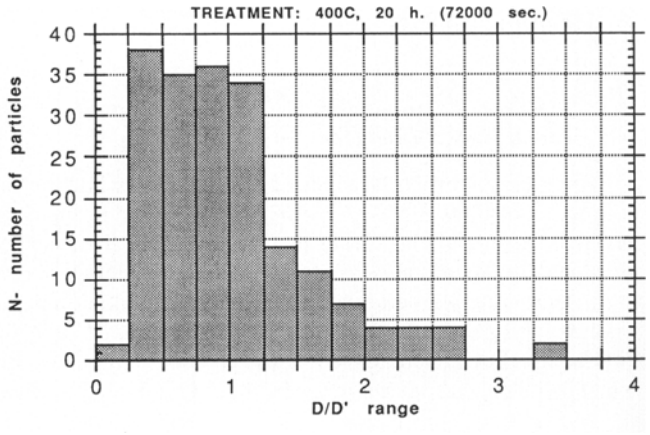

Fig. 6(b) Particle size distribution at alumina fiber interface region of Nextel 610-reinforced Al-224.2 alloy after heat treating to T7 plus 20 h at 400 °C.

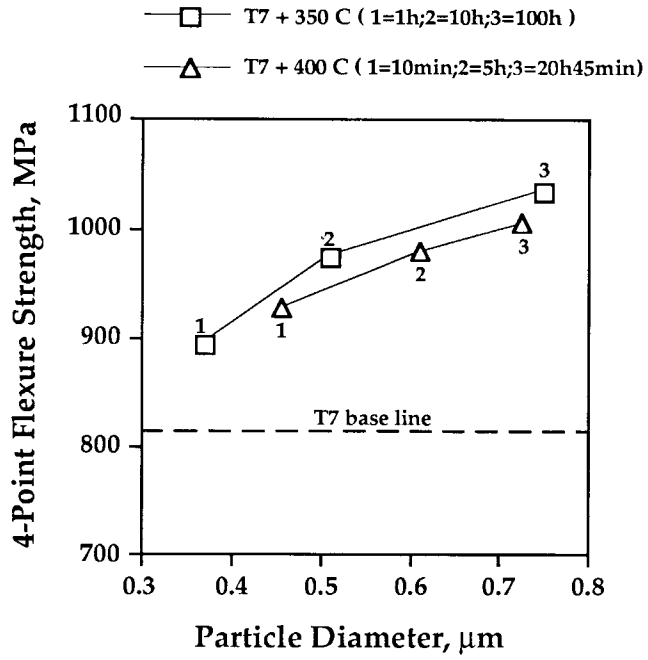

Fig. 7 Flexure strength tests of baseline T7 and companion 350 and 400 °C thermal exposure specimens versus θ particles diameter at the interface.

For the 400 °C reaction, the precipitation stage is complete after ~27 min. The coarsening kinetics at that temperature also follows a $t^{1/4}$ law after the precipitation stage is complete, as shown in Fig. 2(b). The coarsening rate constant of the reaction is higher than for coarsening at the 350 °C isotherm because of the higher grain boundary diffusivity at 400 °C. The plot of interparticle spacing versus exposure time at 400 °C is presented in Fig. 3. The mean free path between particles after ~30 min of exposure also follows a $t^{1/4}$ law.

Particle coarsening at high-angle boundaries should result in a stable particle size distribution, as predicted by theory.[8] The distribution function may be presented as follows:

$$g(u) = \frac{-3\,u^3}{du^4/dt} \exp\left[\int_0^u \frac{3u^3 du}{du^4/dt}\right]$$

where u is the relative particle size ($u = D/D'$); where D' is diameter of the stable particle; and t is time.

The graphic representation of the function for different area fractions of particles from the work of Ardell[8] is presented in Fig. 4. Typical microstructures of the interface region after 27 min and 20 h at 400 °C showing the precipitate sizes and distributions are shown in Fig. 5. To compare the results of the present study with theory, the authors calculated the relative particle size distributions for those thermal exposures at 400 °C. These calculations are presented in Fig. 6(a) and (b). From these figures, it was concluded that the experimental results are contrary to what was expected from the theoretical predictions given in Ref 8. The average particle sizes for both 27 min and 20 h at 400 °C shifted to smaller sizes. Also, there was no threshold limit at larger sizes, which should occur at D/D' values of approximately 1.5 according to Ref 8. The 20-h exposure in the current work does exhibit a shift in distribution toward larger particles compared to the 27-min thermal exposure. The reason for that difference between the current data and the theory of Ref 8 is not clear. However, it may be pointed out that any theoretical treatment of the coarsening problem assumes that the reaction is limited to the grain boundary plain and that equilibrium between the solid solution and precipitates has been established. In the present case, the significantly finer precipitates in the matrix adjacent to the interface region are clearly taking part in the coarsening reaction at the interface. This follows from the fact that the area fraction of precipitates at the interface (21%) vastly exceeds that predicted by the Al-Cu phase diagram. The maximum volume fraction of equilibrium θ is ~7% at room temperature, assuming 5.7% Cu in solid solution during quenching.

3.2 *Mechanical Property Evaluation*

Four-point bend flexure strength tests were performed on specimens heat treated at 350 and 400 °C and T7 heat treated

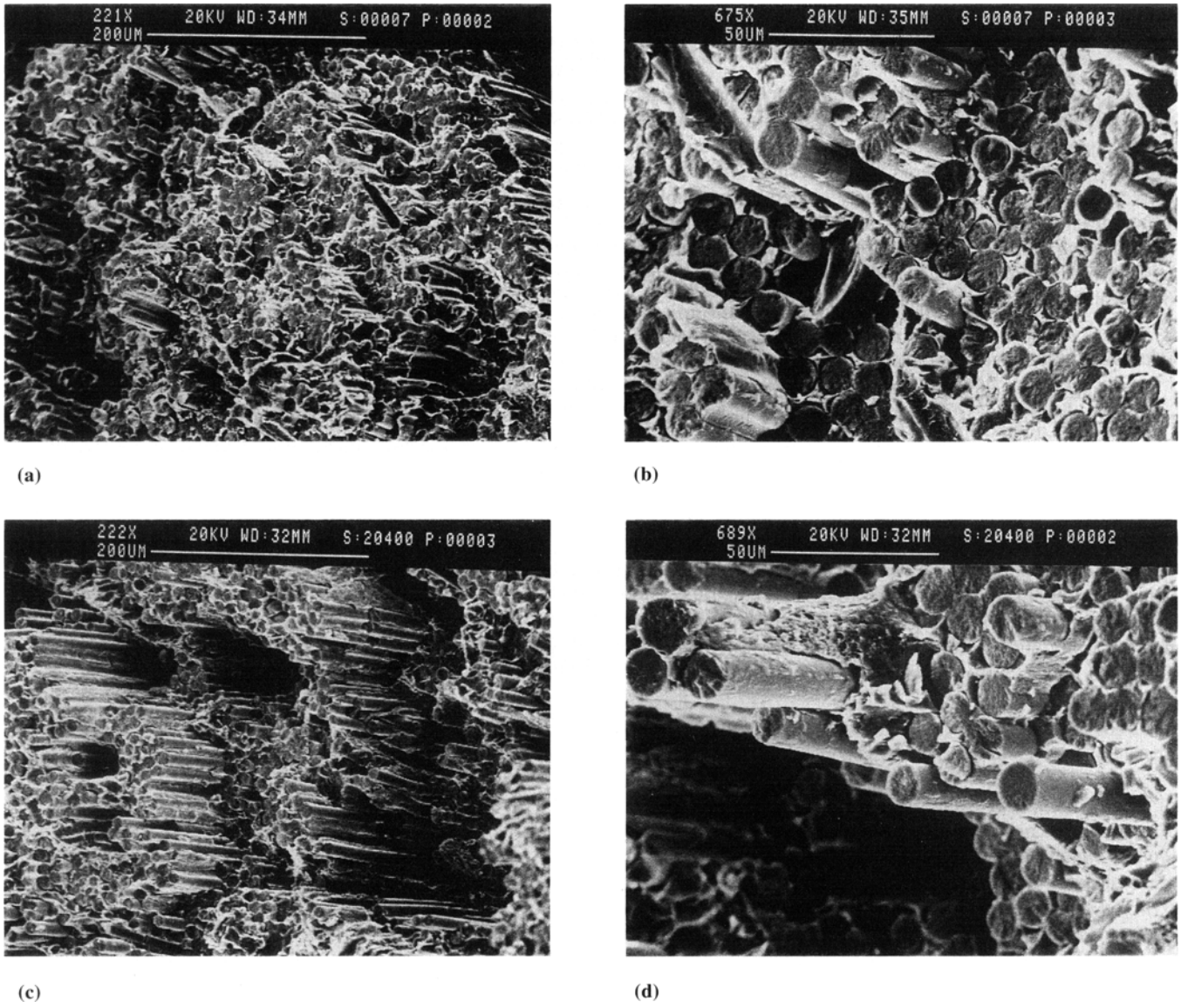

Fig. 8 SEM photomicrographs of tensile region of flexure failure surfaces for specimens heat treated to T7 (a and b) and T7 plus 20 h at 400 °C (c and d).

specimens, which represent the initial condition. The flexure test results in Fig. 7 were related to interfacial precipitate size changes due to thermal exposure. Flexure strength increased with heat treatment time at both isotherms, as shown in Fig. 7. The size of the particles at the fiber/matrix interface clearly governs the strength of the composite by activating the fiber delamination mechanism. The flexure strengths for isoparticle-size materials treated at two different temperatures are similar. The slightly lower strengths for the 400 °C treatment may be due to a lower area fraction of precipitates at the interface (Fig. 2). The specimens heat treated to the maximum times exhibited a nearly 30% increase in flexure strength over the baseline T7 heat treat condition.

The SEM micrographs shown in Fig. 8(c) and (d) illustrate bundled and individual fiber pull-out, indicating that delamination mechanisms are active during fracture of composites subjected to thermal exposure at 400 °C for 20 h. By comparison, the T7 treated specimens are characterized by plainer fracture surface, as shown in Fig. 8(a) and (b).

4. Conclusions

A new algorithm and computer program for determination of average free spacing between neighboring particles was developed and used in the current work. The coarsening of θ precipitates at the Al_2O_3 fiber/224.2 Al matrix alloy interface is governed by a $t^{1/4}$ kinetic rate law at 350 and 400 °C. The interparticle spacing increase obeys a similar $t^{1/4}$ rate law. The particle size distribution as a result of coarsening does not

correspond to theoretical predictions of Ref 8. This has not been explained and should be the subject of further investigation.

Precipitate size and distribution at the fiber/matrix interface govern the process of composite fracture. Heat treatments producing equal particle sizes result in similar flexure strengths. This work confirms the authors' earlier results[3] and conclusions that interfaces discontinuously coated with nonplastically deformable particles can result in composite strengthening and that the control of size and distribution of these particles (or precipitates in the present case) can be used to control the composite mechanical behavior.

Acknowledgments

The materials evaluated at MIT were fabricated by MIT-generated technology as practiced by PCAST under subcontract from the 3M Corporation. This work was a portion of the 3M DARPA funded Model Factory Program under Contract No. MDA972-90-C-0018, with Dr. W. Barker of DARPA serving as Project Manager and Mr. Chauncey Martin serving as Program Manager at 3M. The authors are grateful to the 3M Corporation for donating the fibers used in this study and for waterjet cutting the test coupons from the cast panels. Support for this continuing metallographic evaluation, quantitative metallography, and theoretical evaluations was provided by the IST/SDIO under Office of Naval Research contract N00014-85-K-0645. Additional financial support was also obtained from the Industrial Consortium for Inorganic Composites, which supported a portion of the salary of one of the authors (JC). The authors appreciate the continuing interest of Dr. Steven G. Fishman in these processing and interface related projects.

References

1. V. Gupta, A.S. Argon, and J.A. Cornie, *J. Mater. Sci.*, Vol 24, 1989, p 2031-2040
2. J.A. Cornie, A.S. Argon, and V. Gupta, *Mater. Res. Soc. Bull.*, Vol 16 (No. 4), Apr 1991, p 27-28
3. J.A. Cornie, M.L. Seleznev, M. Ralph, and F.A. Armatis, Jr., Improving Mechanical Properties of Nextel 610 Reinforced Al-224 Alloy through θ Phase Precipitation at the Fiber/Matrix Interface: Part 1, *J. Mater. Sci. Eng.*, in press
4. P.P. Bansal and A.J. Ardell, *Metallography*, Vol 5, 1972, p 97-111
5. P.J. Wray, O. Richmond, and H.L. Morrison, *Metallography*, Vol 16, 1983, p 39-58
6. H.I. Aaronson, C. Laird, and K.R. Kinsman, "Mechanisms of Diffusional Growth of Precipitate Crystals," in *Phase Transformations*, ASM Seminar Proceedings, Oct 12 and 13, 1968, p 313-390
7. H.B. Aaron and H.I. Aaronson, *Acta Metall.*, Vol 16, 1968, p 789
8. A.J. Ardell, On the Coarsening of Grain Boundary Precipitates, *Acta Metall.*, Vol 20, 1972, p 601-609